

Article

Thermally Activated Paramagnets from Diamagnetic Polymers of Biphenyl-3,5-diyl Bis(*tert*-butyl Nitroxides) Carrying Methyl and Fluoro Groups at the 2'- and 5'-Positions

Toru Yoshitake, Hiroki Kudo and Takayuki Ishida *

Department of Engineering Science, The University of Electro-Communications, Chofu, Tokyo 182-8585, Japan; yoshitake@pc.uec.ac.jp (T.Y.); Kudo@pc.uec.ac.jp (H.K.)

* Correspondence: takayuki.ishida@uec.ac.jp; Tel.: +81-42-443-5490; Fax: +81-42-443-5501

Academic Editor: Martin T. Lemaire

Received: 15 February 2016; Accepted: 15 March 2016; Published: 22 March 2016

Abstract: Three new biradicals—2',5'-dimethyl-, 2'-fluoro-5'-methyl-, and 5'-fluoro-2'-methyl-biphenyl-3,5-diyl bis(*tert*-butyl nitroxides)—were synthesized. The magnetic susceptibility measurements revealed their diamagnetism below and around room temperature. The nitroxide groups are located close to each other in an intermolecular fashion to form a weakly covalent head-to-tail (NO)₂ ring. Biradical molecules are connected on both radical sites, constructing a diamagnetic chain. The dimethyl derivative underwent a structural phase transition at 83 °C, clarified via differential scanning calorimetry and powder X-ray diffraction, and a paramagnetic solid phase with *S* = 1 irreversibly appeared. The other analogues exhibited a similar irreversible upsurge of the magnetic susceptibility on heating, but the transition was characterized as the melting.

Keywords: triplet; nitroxide; aminoxyl; spin-polarization; intermolecular coupling; structural phase transition; dimerization

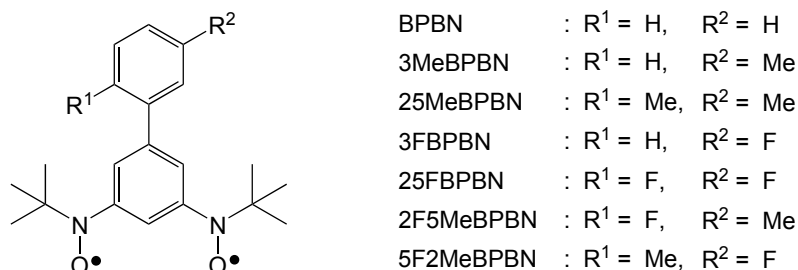
1. Introduction

High-spin organic molecules are realized when nonbonding molecular orbitals are available owing to π -topological symmetry [1–3]. Nitroxide (aminoxyl) chromophores are suitable for the study of intramolecular magnetic coupling because of the persistency; indeed, the low-lying ferromagnetic state has been well established in many *m*-phenylene-bridged bis- and trisnitroxides [4,5]. Biphenyl-3,5-diyl bis(*tert*-butyl nitroxide) (BPBN, Scheme 1) afforded room-temperature triplet materials, owing to the intramolecular ferromagnetic exchange coupling of the order of >300 K [6–11]. More interestingly, intermolecular antiferromagnetic coupling often buried the intramolecular one, giving practically diamagnetic materials and furthermore thermally switchable paramagnetic materials.

Various solid-state magnetic switches are of increasing interest for future applications to sensing, memory, display, and other devices [12]. There have been few known skeletons of organic materials showing facile σ -bond cleavage accompanied by drastic changes of both chromic and magnetic properties. We have reported that the intermolecular N \cdots O σ -type bond is formed and cleaved in the crystals of the BPBN derivatives [6–8,13]. The nitroxide spin centers have a strong tendency to form an intermolecular antiferromagnetic couple or a weak covalent bond. The head-to-tail dimerization of the nitroxide groups is explained in terms of a dipolar character: $>N-O\bullet \leftrightarrow >N^{+\bullet}-O^{-}$ [14–18].

The BPBN system has the advantage of showing intermediate phases in addition to the usual dia- and paramagnetic regimes [7,8]. We have already reported the results on 3'-methylbiphenyl-3,5-diyl bis(*tert*-butyl nitroxide) (3MeBPBN), which displayed the dia-/paramagnetic phase transition at *ca.* 250 K, but the paramagnetic phase has a mere half spin entity [7]. The paramagnetic phase of

a 2',5'-difluoro derivative (25FBPBN) showed only a quarter spin entity, while that of a 3'-fluoro derivative (3FBPBN) exhibited a half [8]. In this study, we concentrate attention to the methyl and fluoro groups at the 2'- and 5'-positions of the biphenyl group. We will report here the results of the structural and magnetic study of 2',5'-dimethyl- and mixed-substituent 2'-fluoro-5'-methyl- and 5'-fluoro-2'-methyl-BPBN derivatives (25MeBPBN, 2F5MeBPBN, and 5F2MeBPBN, respectively).

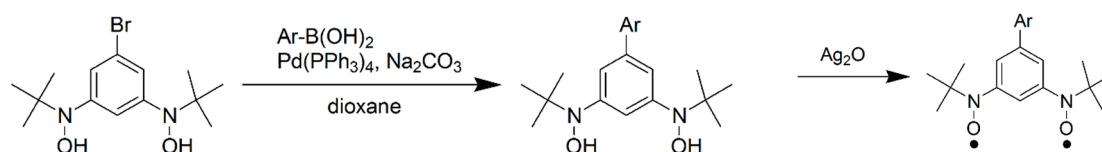


Scheme 1. Structural formula and abbreviations.

2. Results and Discussion

2.1. Preparation and Characterization

Three new biradicals—25Me-, 2F5Me-, and 5F2MeBPBN—were prepared according to Scheme 2 [8]. The Suzuki cross-coupling reaction [19] is a key step, where various commercially available aromatic boronic acids can be coupled with 1-bromo-3,5-bis(*N*-*tert*-butylhydroxylamino)benzene [20]. After the oxidation with Ag₂O, formation of the target biradicals was confirmed by means of solution electron spin resonance (ESR) spectra, which exhibited an unresolved broad line, typical of *m*-phenylene-bridged bisnitroxides [6–11]. The compounds are characterized with elemental analysis and IR spectroscopy. Polymorphs of 25MeBPBN were found; recrystallization from a dichloromethane-hexane mixed solvent in a freezer (−22 °C) gave the α-phase as orange prisms. It turned red at 80–83 °C and melted at 107–109 °C. The β-phase was obtained as red prisms from recrystallization at room temperature, and the mp was 107–109 °C. The mp's of 2F5Me- and 5F2MeBPBN, crystallized from dichloromethane-hexane or hexane, were 71–74 and 85–88 °C, respectively.



Scheme 2. General synthetic route.

2.2. Crystal Structure Analysis

As the X-ray diffraction study at 90–110 K clarifies, they crystallize in a triclinic space group $P\bar{1}$ with $Z = 2$, except for β-25MeBPBN. Table 1 summarizes selected crystallographic data on α-25Me-, β-25Me-, 2F5Me-, and 5F2MeBPBN, together with related known compounds (3Me- and 25FBPBN). The present triclinic compounds are isomorphous (Figure 1a–c, top), and the intermolecular close contacts between O and N atoms are found to be identical (Figure 1a–c, bottom). Although the conformation of the *tert*-butyl nitroxide group is slightly different from those of 3Me-, 3F-, and 25FBPBN, the molecular arrangements are also similar among them. Every nitroxide group is located in very close proximity to each other in an intermolecular fashion, to form a centrosymmetric four-membered (NO)₂ ring from head-to-tail dimerization. The molecules are connected on both radical

sites (Figure 2). As a result, they form a weakly covalent bonded chain running in the crystallographic $b + c$ direction. The intermolecular $O1 \cdots N1^i$ and $O2 \cdots N2^{ii}$ distances are respectively 2.379(3) and 2.348(2) Å for α -25MeBPBN, 2.335(3) and 2.330(4) Å for 2F5MeBPBN, and 2.342(4) and 2.338(6) Å for 5F2MeBPBN, where the symmetry operation codes of i and ii are $(-x, 1 - y, 1 - z)$ and $(-x, -y, -z)$, respectively. They are *ca.* 22%–24% shorter than the sum of the van der Waals radii of O and N atoms (3.07 Å) [21].

Table 1. Selected crystallographic data for BPBN derivatives.

R in RBPBN	3Me	α -25Me	β -25Me	25F	2F5Me	5F2Me
Formula	C ₂₁ H ₂₈ N ₂ O ₂	C ₂₂ H ₃₀ N ₂ O ₂	C ₂₂ H ₃₀ N ₂ O ₂	C ₂₀ H ₂₄ F ₂ N ₂ O ₂	C ₂₁ H ₂₇ FN ₂ O ₂	C ₂₁ H ₂₇ FN ₂ O ₂
T/K	116	90	100	296	100	110
Crystal system	triclinic	triclinic	monoclinic	triclinic	triclinic	triclinic
Space group	$P\bar{1}$	$P\bar{1}$	$C2/c$	$P\bar{1}$	$P\bar{1}$	$P\bar{1}$
$a/\text{Å}$	9.2411(5)	9.184(9)	33.255(8)	9.549(4)	8.888(3)	9.129(3)
$b/\text{Å}$	10.3875(2)	9.5946(1)	5.9206(11)	10.244(5)	9.232(3)	9.246(3)
$c/\text{Å}$	11.7540(5)	12.825(18)	22.178(5)	12.036(5)	12.937(4)	13.074(4)
$\alpha/^\circ$	110.621(4)	112.47(9)	90	111.13(4)	112.68(2)	114.16(2)
$\beta/^\circ$	96.472(3)	91.92(15)	112.325(11)	93.65(3)	92.13(2)	93.73(2)
$\gamma/^\circ$	112.361(4)	106.95(13)	90	116.77(3)	102.80(2)	106.31(2)
$V/\text{Å}^3$	936.09(9)	985(2)	4039.3(16)	943.7(8)	946.2(6)	945.8(6)
Z	2	2	8	2	2	2
$D_{\text{calc}}/\text{g cm}^{-3}$	1.208	1.195	1.166	1.275	1.258	1.259
$\mu(\text{MoK } \alpha)/\text{mm}^{-1}$	0.078	0.076	0.074	0.096	0.087	0.087
$R(F)(I > 2\sigma(I))^a$	0.0595	0.0413	0.0621	0.0689	0.0778	0.1187
$R_w(F^2)(\text{all data})^b$	0.1195	0.0398	0.0906	0.0822	0.1225	0.1626
Goodness-of-fit	1.102	1.003	1.002	0.997	1.023	1.222
No. of reflect.	4175	4280	4606	4292	3831	4297
Reference	Reference [7]	this work	this work	Reference [8]	this work	this work

$$^a R = \sum ||F_o| - |F_c|| / \sum |F_o| \text{ (unit weights); } ^b R_w = [\sum w(F_o^2 - F_c^2)^2 / \sum w(F_o^2)]^{1/2}.$$

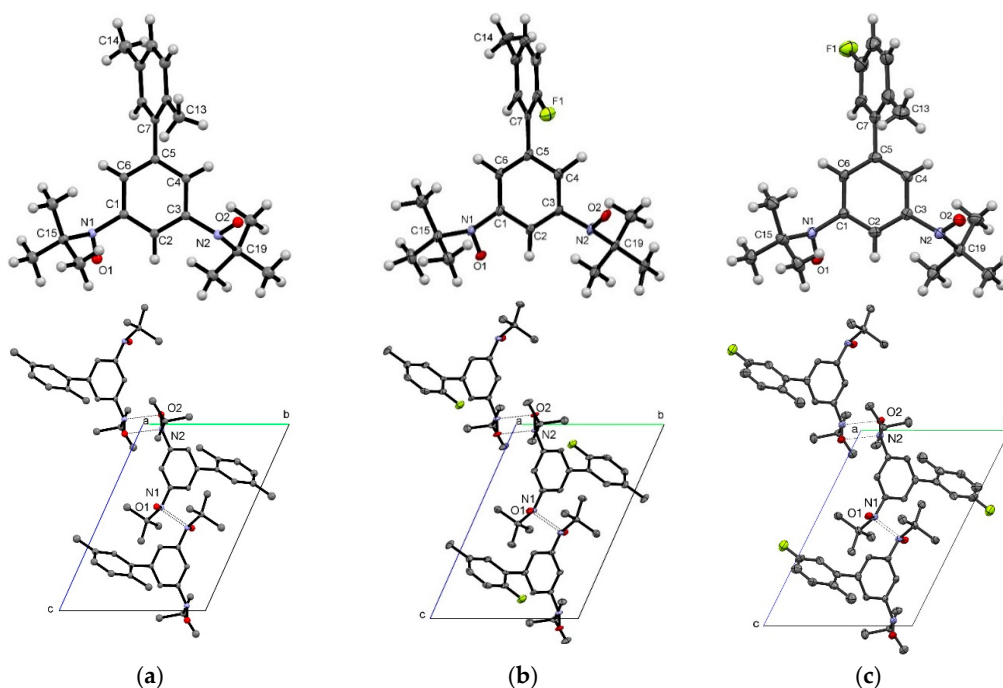


Figure 1. Molecular structure (top) and molecular arrangement (bottom) in the crystals of (a) α -25Me, (b) 2F5Me-, and (c) 5F2MeBPBN. Selected atomic numbering is also shown. Hydrogen atoms are omitted in the bottom panels. Short contacts are denoted with dotted lines.

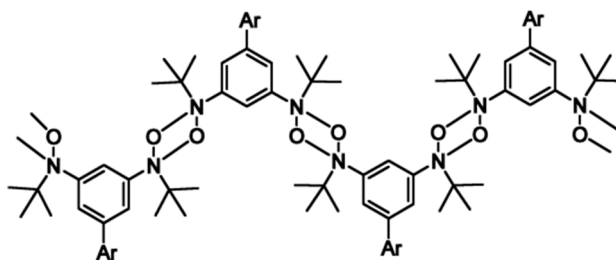


Figure 2. Schematic drawing of the chain involving intermolecular N...O bonds.

Polymorphism of 25MeBPBN was found, and the parameters were satisfactorily refined for both α - and β -phases. As Figure 3 displays, the packing motif of β -25MeBPBN is quite different from that of the α -phase. Intermolecular radical...radical distances are larger than 5.8 Å. The nitrogen atoms possess the sp^2 -hybridized configuration. Such a situation seems to favor $S = 1$ paramagnetism.

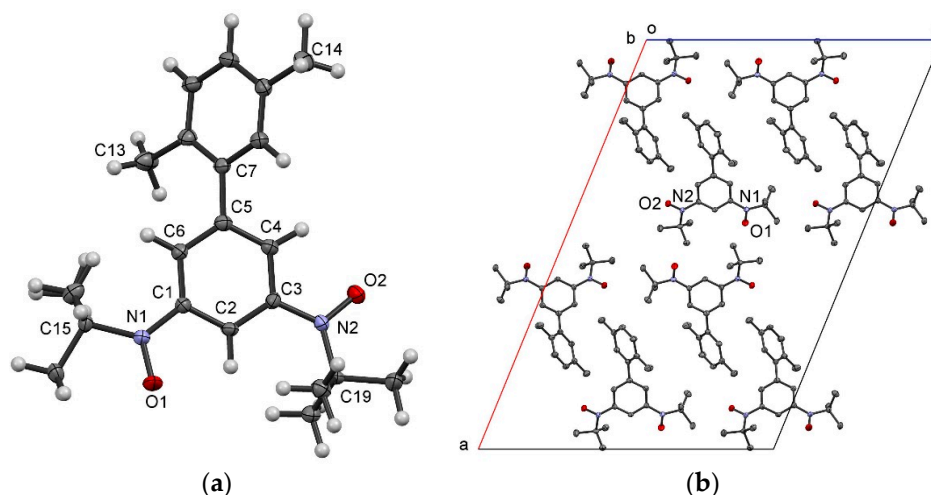


Figure 3. (a) Molecular structure and (b) molecular arrangement in the crystals of β -25MeBPBN. Selected atomic numbering is also shown. Hydrogen atoms are omitted in (b).

The differential scanning calorimetry (DSC; Figure 4) and powder X-ray diffraction (PXRD; Figure 5) of 25MeBPBN clarified that α -25MeBPBN underwent a structural phase transition at 353 K, and β -25MeBPBN irreversibly appeared. The DSC profile of α -25MeBPBN showed two endothermic peaks at 353 and 387 K, whereas that of β -25MeBPBN only one endothermic peak at 387 K. The high-temperature peak is related with the mp. A huge exothermic signal appeared just above the mp, probably ascribable to chemical degradation. The additional peak at 353 K found in α -25MeBPBN is ascribable to a solid-state/solid-state phase transition. The PXRD profile was drastically changed across the transition (Figure 5, bottom and middle). The major PXRD reflections of the high-temperature phase were practically identical to those of the β -25MeBPBN prepared separately (Figure 5, top). A trace of the α -phase was found to remain in the annealed specimen. This finding is entirely consistent with the magnetic study (see below). The $\alpha \rightarrow \beta$ -phase transition was found to be irreversible, as confirmed with the cooling process in the magnetic measurements and DSC analysis. The present observation is similar to that of BPBN [6]. The mother BPBN compound showed the dia-/paramagnetic phase transition accompanied by the $P\bar{1}-C2/c$ space group alteration.

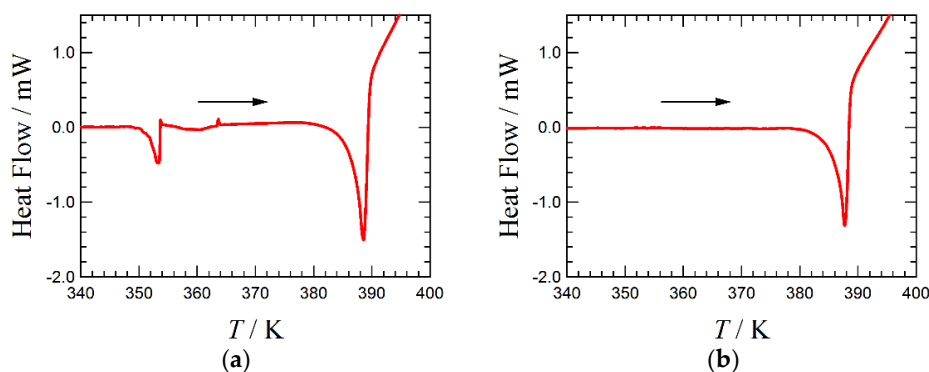


Figure 4. DSC profiles of (a) α - and (b) β -25MeBPBN.

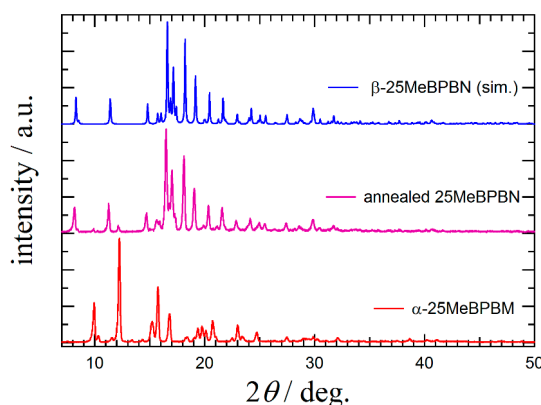


Figure 5. PXRD of three 25MeBPBN specimens; (bottom) α -25MeBPBN as synthesized, (middle) α -25MeBPBN after annealed (recovered after the SQUID thermal-cycle measurements (for details, see Figure 6a)), and (top) a simulation from the data of β -25MeBPBN (The simulation profile was calculated with the room temperature data of β -25MeBPBN as follows: Monoclinic, $C2/c$, $a = 33.431(11)$, $b = 6.092(2)$, $c = 22.342(11)$ Å, $\beta = 112.24(4)^\circ$, $V = 4212(3)$ Å³, $Z = 8$, and $d = 1.118$ g cm⁻³ at $T = 296$ K).

From comparison of the molecular structures of the diamagnetic chains with isolated paramagnetic biradicals [6,9–11] and monoradicals [22–25] previously investigated, the most striking difference is the degree of the nitrogen configuration (hybridization). The nitrogen atoms in polymers display a distinct pyramid because of the tetravalent character (Figure 2), whereas the paramagnetic molecule usually possesses an sp^2 -hybridized planar structure. This finding may imply that the former would have a reduced intramolecular coupling usually accounted for in terms of prohibited π -conjugation. In short, the intermolecular antiferromagnetic coupling interferes with intramolecular ferromagnetic coupling.

2.3. Magnetic Properties

The magnetic susceptibilities of polycrystalline specimens were measured on a Quantum Design SQUID magnetometer (MPMS-XL7). The $\chi_m T$ value of practically null below 350 K for α -25MeBPBN implies the absence of any spin (Figure 6a). In 350–360 K, the $\chi_m T$ value showed an abrupt jump on heating and reached 0.95 cm³·K·mol⁻¹ at 363 K, which is close to the theoretical triplet value (1.00 cm³ K·mol⁻¹) and not to the one expected from twice $S = 1/2$ paramagnetic species (0.75 cm³ K mol⁻¹). The present $\chi_m(T)$ experiment clearly indicates that 25MeBPBN can afford room-temperature triplet material, owing to the intramolecular exchange coupling of the order of >300 K. The spin-polarization mechanism [1–3] is operative, as often verified by *m*-phenylene-bridged biradicals [4,5]. A successive measurement on lowering temperature exhibited a gradual $\chi_m T$ decrease, which can be assigned to an intermolecular antiferromagnetic interaction. The present thermal spin transition at *ca.* 360 K was found to be irreversible, as revealed from repeated measurements.

Figure 6b displays the magnetic susceptibility result on β -MeBPBN prepared separately. The $\chi_m T$ value of $1.0 \text{ cm}^3 \text{ K mol}^{-1}$ at 300 K implies that almost the whole population belongs to the low-lying triplet state, in good agreement with the crystallographic analysis (Figure 3). This $\chi_m T(T)$ profile approximately traced that of annealed α -25MeBPBN (Figure 6a). As described above in the PXRD experiments, annealed α -25MeBPBN was found to be identical to β -25MeBPBN. Thus, we can conclude the one-way phase transition in polymorphic 25MeBPBN.

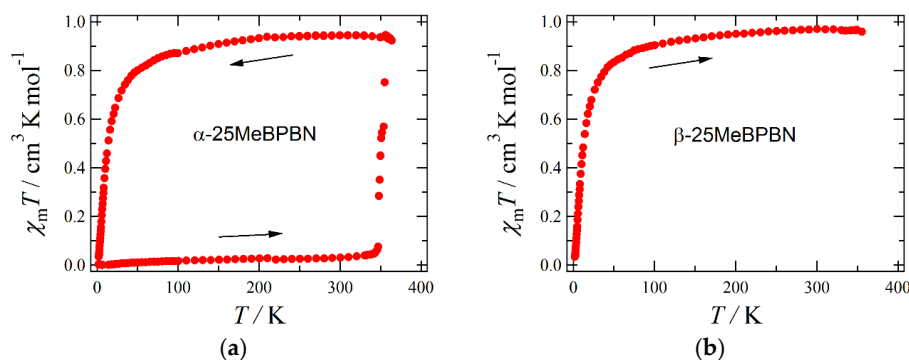


Figure 6. Temperature dependence of $\chi_m T$ measured at 5000 Oe for (a) α -25MeBPBN on heating and then cooling and (b) β -25MeBPBN on heating.

Figure 7 shows the results of 2F5Me- and 5F2MeBPBN, and diamagnetism was recorded below 340 and 350 K, respectively, just like α -25MeBPBN. This finding is consistent with the molecular and crystal structure analysis (Figures 1 and 2). The intermolecular close contact of the nitroxide groups serves as a diamagnetic unit. On heating, appreciable magnetic susceptibility suddenly emerged for both compounds, and the transition was found to be irreversible. The mp's of 2F5Me- and 5F2MeBPBN were 347 and 361 K, respectively, and the melting is supposed to cause the paramagnetism. It is reasonable to infer that weak covalent bonds between the nitroxide groups would cleave into two radicals in the liquid phase.

The $\chi_m T$ values at the end of the transition reached somewhere below $1.0 \text{ cm}^3 \text{ K mol}^{-1}$ (Figure 7) depending on the experimental conditions such as heating rate. A considerable $\chi_m T$ drop was observed when the specimen was kept in the melt. This behavior was confirmed for 2F5Me- and 5F2MeBPBN by means of ESR spectroscopy. A variable-temperature ESR technique was applied to the solid specimens, and the biradical signals were found to decrease while being allowed to stand above the mp (Figure 8 for 5F2MeBPBN). These findings indicate that the melted 2F5Me- and 5F2MeBPBN were chemically decomposed under such thermal conditions. The *m*-phenylene-bridged bisnitroxides are known to thermally change into isomeric diamagnetic compounds, aminoquinone imine *N*-oxide derivatives [6,10,26,27].

In contrast, all the BPBN biradical species in the solid phase were persistent enough. In the present study, the $\chi_m T$ value of the annealed α -25MeBPBN indicates negligible decomposition. This finding is compatible with the notion that 25MeBPBN undergoes the spin transition entirely in the solid phase.

We found the solid-state/solid-state structural phase transition only in 25MeBPBN. The transition temperature was $83 \text{ }^\circ\text{C}$ in a melting point apparatus ($87 \text{ }^\circ\text{C}$ in SQUID and $80 \text{ }^\circ\text{C}$ in DSC), which is considerably lower than the mp ($109 \text{ }^\circ\text{C}$ for the β -phase). Application in electronics and devices may welcome a solid-state structural phase transition taking place near room temperature. The fluoro group is smaller and more electronegative than the methyl group, and the substitution of Me with F may lead to increase the intermolecular contact, which is supported by the density (Table 1). Such contacts assist the cooperativity [8,12], but unfortunately in the present case the reduction of the void space may be unfavorable for the substituent motion. Consequently, no solid-state phase transition is realized before the melting for 2F5Me- and 5F2MeBPBN.

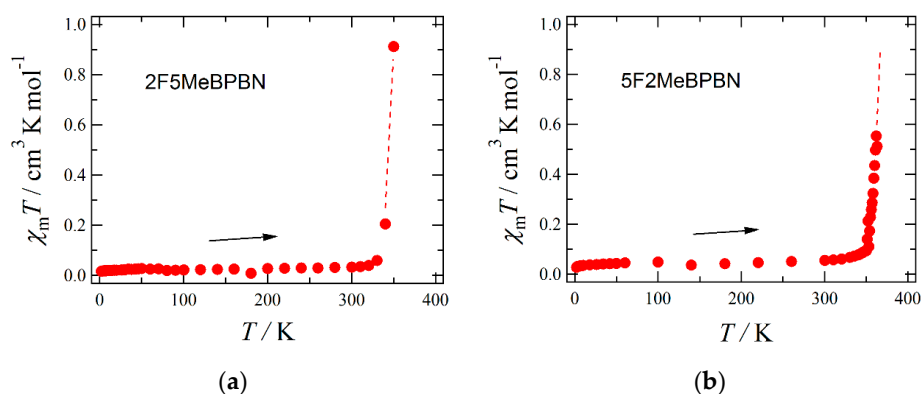


Figure 7. Temperature dependence of $\chi_m T$ for (a) 2F5Me- and (b) 5F2MeBPBN, measured at 5000 Oe on heating from 2 to 350 and 360 K, respectively. Dotted lines are shown for a guide to the eye.

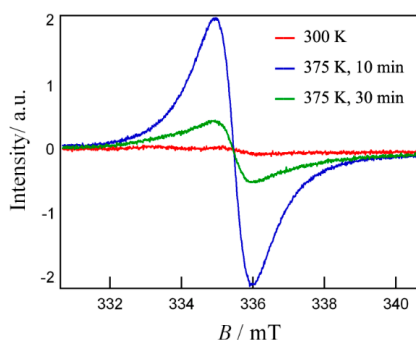


Figure 8. ESR spectra of 5F2MeBPBN, measured in the following sequence: (1) a solid state at 300 K, (2) a liquid state after being kept at 375 K for 10 min and (3) at the same temperature after 30 min.

3. Experimental Section

3.1. Preparation of BPBN Derivatives

The compounds presented here were prepared according to a known procedure [8], using commercially available 2,5-dimethyl-, 2-fluoro-5-methyl-, and 5-fluoro-2-methylbenzene boronic acids. The yields of the Suzuki coupling reactions are 55%, 47% and 20%, respectively. The Ag_2O oxidation gave the target biradicals in 50%, 77% and 89% yields for 25Me-, 2F5Me-, and 5F2MeBPBN, respectively. Anal. Calcd. for 25MeBPBN ($\text{C}_{22}\text{H}_{30}\text{N}_2\text{O}_2$): C, 74.12%; H, 9.05%; N, 7.86%. Found: C, 74.15%; H, 9.01%; N, 7.64%. MS (ESI, MeOH) m/z 377.22 ($\text{M} + \text{Na}^+$). IR (neat, attenuated total reflection (ATR)) α -phase: 2987, 2942, 1552, 1464, 1340, 1238, 1186, 879, 818, 740, 684, 523, 468, 441 cm^{-1} ; β -phase: 2987, 2964, 1574, 1481, 1446, 1357, 1282, 1183, 859, 818, 747, 701, 562, 493, 413 cm^{-1} . For selective preparation of the α - and β -phases, see Section 2.1. Anal. Calcd. for 2F5MeBPBN ($\text{C}_{21}\text{H}_{27}\text{F}_1\text{N}_2\text{O}_2$): C, 70.37%; H, 7.59%; N, 7.82%. Found: C, 70.39%; H, 7.92%; N, 7.89%. MS (ESI, MeOH) m/z 381 ($\text{M} + \text{Na}^+$). IR (neat, ATR) 2988, 2966, 1596, 1497, 1480, 1387, 1233, 1179, 818, 746 cm^{-1} . Anal. Calcd. for 5F2MeBPBN ($\text{C}_{21}\text{H}_{27}\text{F}_1\text{N}_2\text{O}_2$): C, 70.37%; H, 7.59%; N, 7.82%. Found: C, 70.04%; H, 7.90%; N, 7.83%. MS (ESI, MeOH) m/z 381 ($\text{M} + \text{Na}^+$). IR (neat, ATR) 2967, 2931, 1595, 1495, 1422, 1400, 1245, 1210, 824, 744 cm^{-1} .

3.2. Crystallographic Analysis

X-Ray diffraction data were collected on a Saturn70 CCD diffractometer (Rigaku, Tokyo, Japan) with graphite monochromated Mo $\text{K}\alpha$ radiation ($\lambda = 0.71073 \text{ \AA}$). The structures were directly solved by a heavy-atom method and expanded using Fourier techniques in the CRYSTALSTRUCTURE [28]. Numerical absorption correction was used. The thermal displacement

parameters of non-hydrogen atoms were refined anisotropically. Selected crystallographic data are listed in Table 1. CCDC numbers 1452767–1452770 contain the supplementary crystallographic data for α -25Me-, β -25Me-, 2F5Me-, and 5F2MeBPBN. These data can be obtained free of charge via <http://www.ccdc.cam.ac.uk/conts/retrieving.html>. The powder X-ray diffraction patterns (PXRD) were recorded on an Ultima III diffractometer (Rigaku, Tokyo, Japan) using CuK α radiation ($\lambda = 1.54178 \text{ \AA}$).

3.3. Physical Property Measurements

Magnetic susceptibilities were measured on an MPMS-XL7 SQUID (Quantum Design, San Diego, CA, USA) magnetometer with a static field of 0.5 T. The magnetic responses were corrected with diamagnetic blank data of the sample holder measured separately. The diamagnetic contribution of the sample itself was estimated from Pascal's constants [29]. The electron spin resonance (ESR) spectra were recorded on an ELEXYS ESR spectrometer (Bruker, Billerica, MA, USA) with an X-band gun oscillator. A diluted toluene solution or polycrystalline solid of the specimen was degassed before measurements. The differential scanning calorimetry (DSC) of 25FBPBN was performed on a Rigaku Thermo Plus DSC 8230 (Rigaku, Tokyo, Japan). The heating rate was 1 deg/min.

4. Conclusions

The magnetic susceptibility measurements of new biradicals 25MeBPBN, 2F5MeBPBN, and 2Me5FBPBN practically showed diamagnetism below room temperature. The radical dimerization occurs on both sides of the biradical, thus leading to polymerization. All three showed thermally activated paramagnetism due to the degradation, but only 25MeBPBN underwent a solid-state structural phase transition before the melting. Electronics-oriented applications may welcome a solid-state structural phase transition taking place near room temperature. For example, the present biradicals underwent one-way thermally activated transition, being regarded as a potential candidate for write-once media in information storage devices. Crystal engineering approaches are important to control weak intermolecular interaction, acquire a void space in the crystal, and tune the phase transition phenomena.

Acknowledgments: This work was financially supported from KAKENHI (JSPS/15H03793).

Author Contributions: Toru Yoshitake and Hiroki Kudo participated in the preparation, X-ray structural analysis, and magnetic study. Takayuki Ishida designed the study and wrote the manuscript.

Conflicts of Interest: The authors declare no conflict of interest.

References

1. Iwamura, H. What role has organic chemistry played in the development of molecule-based magnets? *Polyhedron* **2013**, *66*, 3–14. [[CrossRef](#)]
2. Gallagher, N.M.; Olankitwanit, A.; Rajca, A. High-spin organic molecules. *J. Org. Chem.* **2015**, *80*, 1291–1298. [[CrossRef](#)] [[PubMed](#)]
3. Blundell, S.J.; Pratt, F.L. Organic and molecular magnets. *J. Phys. Condens. Matter* **2004**, *16*, R771–R828. [[CrossRef](#)]
4. Mukai, K.; Nagai, H.; Ishizu, K. The proof of a triplet ground state in the *N,N'*-di-*t*-butyl-*m*-phenylenebisnitroxide biradical. *Bull. Chem. Soc. Jpn.* **1975**, *48*, 2381–2382. [[CrossRef](#)]
5. Ishida, T.; Iwamura, H. Bis[3-*tert*-butyl-5-(*N*-oxy-*tert*-butylamino)phenyl] nitroxide in a quartet ground state: A prototype for persistent high-spin poly[(oxyimino)-1,3-phenylenes]. *J. Am. Chem. Soc.* **1991**, *113*, 4238–4241. [[CrossRef](#)]
6. Nishimaki, H.; Mashiyama, S.; Yasui, M.T.; Nogami, T.; Ishida, T. Bistable polymorphs showing diamagnetic and paramagnetic states of an organic crystalline biradical biphenyl-3,5-diyl bis(*tert*-butylnitroxide). *Chem. Mater.* **2006**, *18*, 3602–3604. [[CrossRef](#)]

7. Nishimaki, H.; Ishida, T. Organic two-step spin-transition-like behavior in a linear $S = 1$ array: 3'-methylbiphenyl-3,5-diyl bis(*tert*-butylnitroxide) and related compounds. *J. Am. Chem. Soc.* **2010**, *132*, 9598–9599. [[CrossRef](#)] [[PubMed](#)]
8. Konno, T.; Kudo, H.; Ishida, T. Intermediate-paramagnetic phases with a half and a quarter spin entities in fluorinated biphenyl-3,5-diyl bis(*tert*-butyl nitroxides). *J. Mater. Chem. C* **2015**, *3*, 7813–7818. [[CrossRef](#)]
9. Kawakami, H.; Tonegawa, A.; Ishida, T. A designed room-temperature triplet ligand from pyridine-2,6-diyl bis(*tert*-butyl nitroxide). *Dalton Trans.* **2015**, *45*, 1306–1309. [[CrossRef](#)] [[PubMed](#)]
10. Kawakami, H.; Tonegawa, A.; Ishida, T. Pyridine-2,6-diyl dinitroxides as room-temperature triplet ligands. *AIP Conf. Proc.* **2016**, *1709*, 020017.
11. Yoshitake, T.; Ishida, T. Ferromagnetic chains of ground triplet 5-methoxy-1,3-phenylene bis(*tert*-butyl nitroxide). *Chem. Lett.* **2016**. [[CrossRef](#)]
12. Gütllich, P., Goodwin, H.A., Eds.; *Spin Crossover in Transition Metal Compounds I, II, and III*; Springer: Berlin, Germany, 2004.
13. Kurokawa, G.; Ishida, T.; Nogami, T. Remarkably strong intermolecular antiferromagnetic couplings in the crystal of biphenyl-3,5-diyl bis(*tert*-butyl nitroxide). *Chem. Phys. Lett.* **2004**, *392*, 74–79. [[CrossRef](#)]
14. Marsh, D. Reaction fields and solvent dependence of the EPR parameters of nitroxides: The microenvironment of spin labels. *J. Mag. Res.* **2008**, *190*, 60–67. [[CrossRef](#)] [[PubMed](#)]
15. Kanzaki, T.; Shiomi, D.; Sato, K.; Takui, T. Biradical paradox revisited quantitatively: A theoretical model for self-associated biradical molecules as antiferromagnetically exchange coupled spin chains in solution. *J. Phys. Chem. B* **2012**, *116*, 1053–1059. [[CrossRef](#)] [[PubMed](#)]
16. Matsumoto, S.; Higashiyama, H.; Akutsu, H.; Nakatsuji, S. A functional nitroxide radical displaying unique thermochromism and magnetic phase transition. *Angew. Chem. Int. Ed.* **2011**, *50*, 10879–10883. [[CrossRef](#)] [[PubMed](#)]
17. Capiomont, A.; Chion, B.; Lajzerowicz, J. Affinement de la structure du radical nitroxyde dimerisé: bicycle [3,3,1] nonanone-3 aza-9 oxyle-9. *Acta Cryst. B* **1971**, *27*, 322–326. [[CrossRef](#)]
18. Ishida, T.; Ooishi, M.; Ishii, N.; Mori, H.; Nogami, T. Mono- and dinitroxide radicals from 9, 9'(10*H*, 10'*H*)-spirobiacridine: An approach to a D_{2d} triplet biradical. *Polyhedron* **2007**, *26*, 1793–1799. [[CrossRef](#)]
19. Suzuki, A. Cross-coupling reactions of organoboranes: An easy way to construct C-C bonds (Nobel lecture). *Angew. Chem. Int. Ed.* **2011**, *50*, 6722–6737. [[CrossRef](#)] [[PubMed](#)]
20. Kanno, F.; Inoue, K.; Koga, N.; Iwamura, H. Persistent 1,3,5-benzenetriyl tris(*N*-*tert*-butyl nitroxide) and its analogs with quartet ground states. Intramolecular triangular exchange coupling among three nitroxide radical centers. *J. Phys. Chem.* **1993**, *97*, 13267–13272. [[CrossRef](#)]
21. Bondi, A. van der Waals volumes and radii. *J. Phys. Chem.* **1964**, *68*, 441–451. [[CrossRef](#)]
22. Koide, K.; Ishida, T. Biradical chelating host 2,2'-bipyridine-6,6'-diyl bis(*tert*-butyl nitroxide) showing tunable exchange magnetic coupling. *Inorg. Chem. Commun.* **2011**, *14*, 194–196. [[CrossRef](#)]
23. Osada, S.; Hirokawa, N.; Ishida, T. Polyether-bridged bis(*tert*-butyl nitroxide) paramagnetic hosts showing receptor ability to calcium(II) and barium(II) ions. *Tetrahedron* **2012**, *68*, 6193–6197. [[CrossRef](#)]
24. Konno, T.; Koide, K.; Ishida, T. A supramolecular switch between ground high- and low-spin states using 2,2':6',2''-terpyridine-6,6''-diyl bis(*tert*-butyl nitroxide). *Chem. Commun.* **2013**, *49*, 5156–5158. [[CrossRef](#)] [[PubMed](#)]
25. Okazawa, A.; Nagaichi, Y.; Nogami, T.; Ishida, T. Magneto-structure relationship in copper(II) and nickel(II) complexes chelated with stable *tert*-butyl 5-phenyl-2-pyridyl nitroxide and related radicals. *Inorg. Chem.* **2008**, *47*, 8859–8868. [[CrossRef](#)] [[PubMed](#)]
26. Calder, A.; Forrester, A.R.; James, P.G.; Luckhurst, G.R. Nitroxide radicals. V. *N,N'*-Di-*t*-butyl-*m*-phenylenebinitroxide, a stable triplet. *J. Am. Chem. Soc.* **1969**, *91*, 3724–3727.
27. Forrester, A.R.; Thompson, R.H. Stable nitroxide radicals. *Nature* **1964**, *203*, 74–75. [[CrossRef](#)]
28. *CRYSTALSTRUCTURE, version 4.2*; Rigaku/MS: The Woodlands, TX, USA, 2015.
29. Kahn, O. *Molecular Magnetism*; VCH Publishers, Inc.: Weinheim, Germany, 1993; pp. 257–261.

